PACS: 81.40.Lm, 62.20.Fe

S.V. Dobatkin

NANOCRYSTALLINE STRUCTURES IN Al- AND Fe-BASED ALLOYS AFTER SEVERE PLASTIC DEFORMATION

Moscow State Steel and Alloys Institute (Technological University)
Leninsky prospekt, 4, 117936 Moscow, Russia

E-mail: dobatkin@tmo.misa.ac.ru

Formation of ultrafine-grained structure in metals and alloys during severe plastic deformation (SPD) at low temperature is established well known. But not always the nanoscale structure can be obtained. This work shows the possibility of additional refinement of structure up to nanocrystalline state (grain size less than 100 nm) in Al- and Fe-based alloys due to phase transformations during SPD by torsion under high pressure.

1. Introduction

Severe shear plastic deformation is one of the most effective ways to produce non-porous and bulk samples with ultrafine (nano- and submicrocrystalline) structure [1–3]. The specific structure is characterized by high concentration of boundaries of structural elements and their non-equilibrium condition, causes singularity of both mechanical [3,4] and physical [3,5] properties.

Formation of ultrafine-grained structure in metals and alloys during severe plastic deformation (SPD) at low temperature is well known. But not always the nanoscale structure can be obtained.

At the same time, during cold deformation some phase transformations were observed [6,7].

So, the purpose of the present work is to examinate a possibility of additional refinement of the structure up to nanoscale size in Al- and Fe-based alloys during SPD by torsion under high pressure due to phase transformation.

2. Experimental Procedure

As materials of research were chosen Al-based alloys: Al–Cu–Mg-alloy 2024 (4.2% Cu; 1.6% Mg) [8] and Al–Mg–Sc-alloy 01570 (5.9% Mg; 0.3 % Sc; 0.18% Zr) [9], and steels: austenitic 08Cr18Ni10Ti (0.08% C; 18.3% Cr; 9.8% Ni; 0.6% Ti) [10] and 05Cr15Ni9Cu2TiNMoV (0.04% C; 14.3% Cr; 9.5% Ni; 0.2% V; 2.0% Cu; 1.4% Mo; 0.04% Ti; 0.1% N) [10], ferritic 08Cr18Ti (0.08% C; 18.4 % Cr; 0.6% Ti) [10] and ferritic-pearlitic 10Mn2VTi (0.09% C; 1.6% Mn; 0.08% Ti; 0.1% V).

Deformation was performed by torsion under pressure of 6 GPa on a Bridgman-type device. The samples of 10 mm in diameter and 1 mm in thickness were previously 50% deformed by compression and later by torsion to different strains up to 9 revolutions which corresponds to logarithmic strain on a half of the sample radius $e = 6.4$ [11].

The structure analysis has been carried out using a transmission electron microscope JEM-100X. DRON-3 diffractometer was used for X-ray analysis. Microhardness was defined using a PMT-3 device with 50 g load.

3. Severe plastic deformation of Al-based alloys

3.1. Results

Al–Cu–Mg-alloy

It is known that the formation of submicrocrystalline structure in aluminium alloys during severe plastic deformation at room temperature results in significant strengthening. But an opportunity of additional strengthening at the expense of aging in submicrocrystalline matrix at severe shear deformation of quenched aluminium alloy is not practically investigated.

The microhardness of 2024 alloy in the initial as-hot-pressed state as well as after quenching had approximately the same value of ~ 0.8 GPa (Fig. 1). After quenching with subsequent natural aging the microhardness was 1.2 GPa.

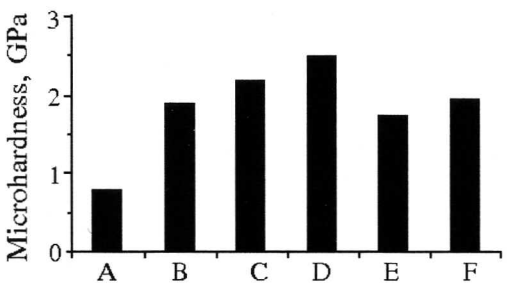

Fig. 1. Microhardness of Al–Cu–Mg-alloy 2024 after different routes of thermal treatment and severe plastic deformation (SPD): A – quenching, B – SPD at 20°C of hot-pressed state, C – SPD at 20°C of quenched state, D – regime C + natural aging, E – SPD at 200°C of quenched state, F – SPD at 20°C of quenched and pre-aged state

Room-temperature deformation of initial non-quenched (hot-pressed) specimens leads to strong hardening. With increasing strain the microhardness grows and almost attains the steady-state value of 1.9 GPa at $e = 6.8$ (5 revolutions).

Room-temperature deformation of quenched specimens was accompanied by microhardness increase to 2.2 GPa [8]. Subsequent holding at $T = 20$°C for four days resulted in further hardening up to $H_\mu = 2.4$ GPa. Deformation of quenched specimens at the temperature of artificial aging (200°C) led to lower hardening (after natural aging), $H_\mu = 1.8$ GPa, than deformation at room temperature, $H_\mu = 2.2$ GPa (Fig. 1).

The attempts were made to deform partially aged alloy with initial microhardness of 1.4 GPa after quenching and natural aging for two days. In this case the final hardening after deformation and natural aging is lower ($H_\mu = 1.9$ GPa) than after deformation of as-quenched alloy ($H_\mu = 2.4$ GPa).

TEM of non-quenched and quenched specimens deformed at room temperature to $e = 6.8$ (5 revolutions) revealed ultrafine grain structure with predominantly high-angle boundaries (Fig. 2) [8]. Average grain size obtained from dark-field images was ~ 150 nm for as-hot-pressed specimen (Fig. 2,*b*) and ~ 50 nm for as-quenched specimen (Fig. 2,*a*).

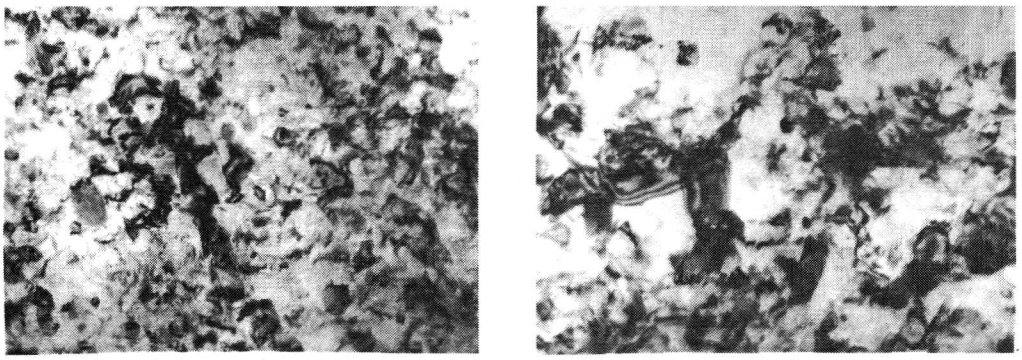

a *b*

Fig. 2. Structure of Al–Cu–Mg-alloy 2024 after SPD with e = 6.8 at 20°C (initial state: *a* – quenched, *b* – hot-pressed)

Al–Mg–Sc-alloy

The increased interest to ultrafine grained Al–Sc-alloys is caused by an opportunity of realization of high-speed and low-temperature superplasticity in them and a prospect of using these alloys in the aerospace industry. In the present work a possibility of nanocrystalline structure obtaining in Al–5.9%Mg–0.3%Sc–0.18%Zr-alloy during severe plastic deformation is investigated [9].

Room-temperature deformation of as-hot-pressed Al–Mg–Sc-alloy leads to double increase in microhardness from 1.2 to 2.4 GPa. Steady state H_μ-values are attained at e = 6.8 (5 revolutions).

During severe deformation at T = 200°C with e = 6.8 (5 revolutions) the hardening remains high. With temperature increasing to 400°C it decreases but to initial values (Fig. 3).

Heating after cold deformation to 200°C does not practically change microhardness (Fig. 4). With heating to 400°C microhardness decreases almost to its initial values (Fig. 4).

TEM analysis revealed nanocrystalline structure after deformation at T = 20°C and e = 6.8 (5 revolutions) with average grain size of 50 nm and predominantly high-angle boundaries (Fig. 5,*a*) [9]. After deformation at 200°C and ε = 6.8 (5 revolutions) the

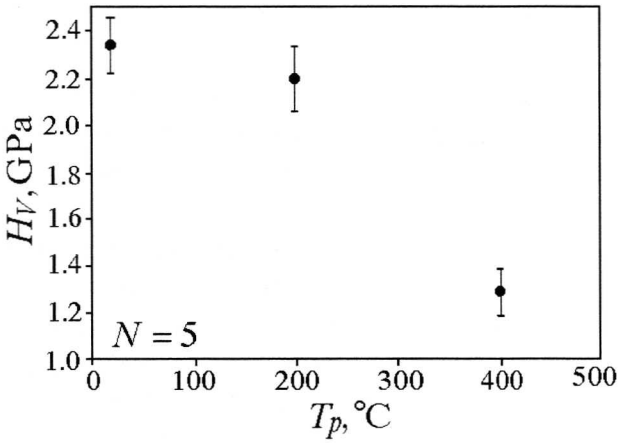

Fig. 3. Microhardness dependence on the processing temperature during SPD (5 turns)

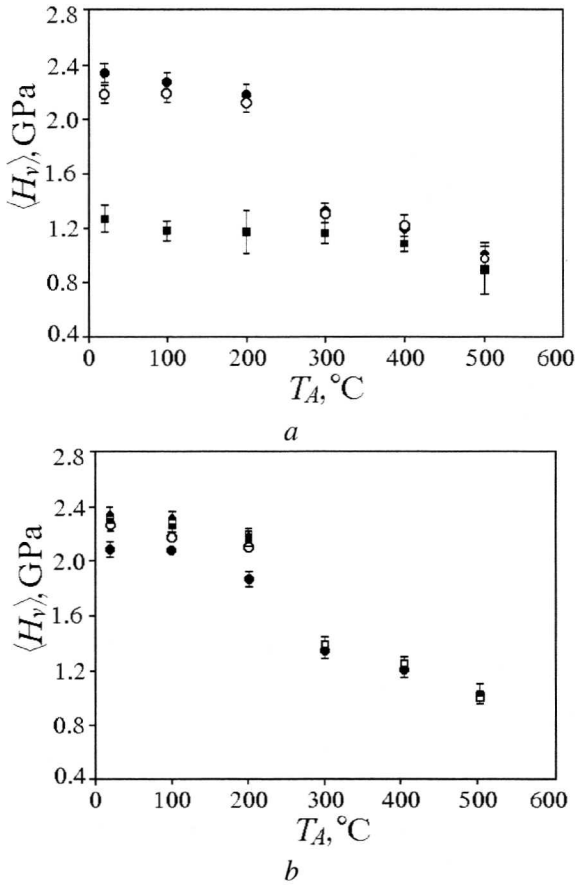

Fig. 4. Microhardness dependence on the annealing temperature after SPD: *a* – temperature of processing T_p, °C: ● – 20, o – 200, ■ – 400, strain N = 5 turns; *b* – T_p = 20°C, strain, turns: ● – 1, o – 3, ■ – 5, □ – 7, ▲ – 10

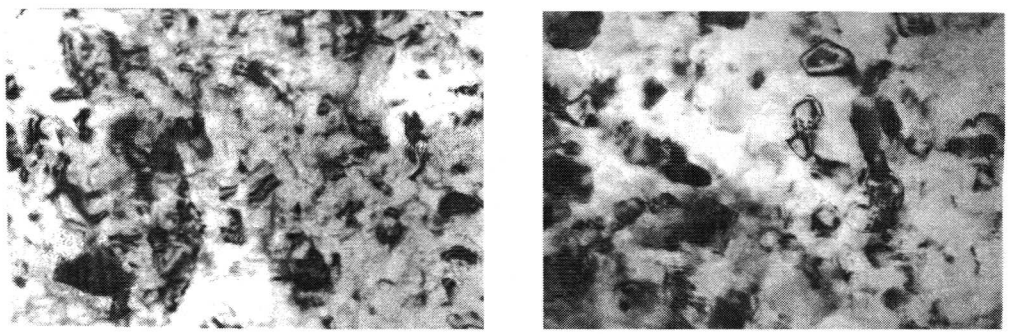

Fig. 5. Structure of Al–Cu–Mg-alloy 01570 after SPD by torsion with e = 6.8 at 20°C (*a*) and 400°C (*b*)

average grain size grows to 90 nm and reaches 200–300 nm after deformation at 400°C (Fig. 5,*b*).

Heating of nanocrystalline structure with initial grain size of 50 nm (after deformation at 200°C with e = 6.8 (5 revolutions)) up to 200°C leads to slight growth to 90 nm. Heating up to 400°C results in significant grain growth to ~ 1 μm.

3.2. Discussion

Al–Cu–Mg-alloy

In the absence of phase transformations a considerable hardening of as-hot-pressed Al–Cu–Mg-alloy after intensive cold deformation is most likely to occur due to large grain boundary area of submicrocrystalline structure with average grain size of ~ 150 nm (see Fig. 2,*b*).

Deformation of as-quenched alloy at T = 20°C results in final grain size of 50 nm and higher hardening (see Fig. 1, 2,*a*). It is reasonable to assume that the deformation of oversaturated solid solution facilitates precipitation of θ′- and S′-phases even during deformation, that is, in other words, facilitates strain aging [8].The latter leads to hardening due to both dispersed particles and grain refinement caused by these particles. Strain aging does not come to its completion and subsequent natural aging results in additional hardening (see Fig. 1).

Severe deformation of Al–Cu–Mg-alloy at 200°C, i.e. in the temperature range of artificial aging, produces lower hardening than cold deformation (see Fig. 1). This can be regarded as an evidence for a strain-induced shift of aging temperature.

Severe deformation of as-quenched or partially aged Al–Cu–Mg-alloy also leads to a lower hardening than the deformation of freshly quenched alloy (see Fig. 1). Consequently, the maximum grain refinement can be obtained by deformation of alloy with maximum extent of oversaturation of solid solution.

Therefore, severe deformation of oversaturated solid solution of Al–Cu–Mg-alloy allows to overcome the nanoscale of grain size (≤ 100 μm) due to overlapping of phase transformations and to obtain nanocrystalline structure with grain size of ~ 50 μm.

Al–Mg–Sc-alloy

The torsion strain dependencies of microhardness are similar for both studied alloys, but in case of Al–Mg-alloy with Sc additions the absolute values of microhardness are higher. For both alloys microhardness attains its maximum at ε = 6.8 (5 revolutions) and does not change with further increase of strain. This could be considered as an indirect indication of similarity of microstructures deformed at T = 20°C with $e \geq 6.8$ (5 revolutions).

The drawback of nanostructural materials is their low thermal stability. Heating of nanostructured Al–Mg–alloy with Sc additions after SPD to 200°C is accompanied by a slight grain growth (~ 90 nm) and by a slight decrease in microhardness (see Fig. 4). With heating to 400°C the grain growth becomes much more pronounced (~ 1 μm). While after heating to 200°C it was fairly difficult to correctly determine the size of Al_3Sc particles from dark-field TEM images due to specific peculiarities of electron diffraction patterns arising from fine grain size, no difficulties were faced in case of heating to 400°C. The particle average size was more than 70 nm. The particles of such a size cannot already inhibit the grain boundary migration [12].

SPD of Al–Mg–Sc-alloy at 200°C leads to nanocrystalline structure with average grain size of ~ 90 nm. As indicated by TEM studies and microhardness, this state of

microstructure is similar to that obtained after heating the cold-worked alloy to 200°C (see Fig. 3, 4). In the latter case the microhardness and grain size are close to those after room-temperature SPD.

SPD at 400°C results in average grain size of 200–300 nm [9]. This small grain size obtained in hot deformation cannot be explained only by deformation conditions. Most likely, despite the decomposition of Sc solid solution in Al after annealing the remaining Sc precipitates as Al_3Sc particles that stabilize grain boundaries.

Thus, the addition of Sc to Al–Mg-alloy allows to obtain nanocrystalline structure after SPD at temperatures up to 200°C. At this temperature less non-equilibrium grain boundaries and, consequently, higher ductility can be anticipated.

4. Severe plastic deformation of steels

Low-carbon steels

The present work was aimed to study the formation of UFG-structure (< 100 nm) in low-carbon steels during SPD by torsion under pressure at the expense of deformation of non-equilibrium state. 10Mn2VTi steel was either hot-rolled or quenched prior to room-temperature torsion.

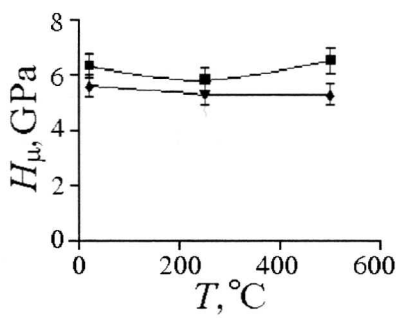

Fig. 6. Microhardness of low-carbon steel 10G2FT after SPD with e = 6.8 and T = 20–500°C: ■ – quenched initial state; ▲ – hot-rolled initial state

For both states, microhardness after deformation did not change in the temperature range of 20–500°C, with microhardness of the quenched steel being always higher (Fig. 6). This might be attributed to the presence of bainite, smaller final grain size, decomposition of solid solution and precipitation of fine carbides.

TEM study of initially quenched and deformed steel revealed cells and grains with average size below 100 nm. With temperature increasing to 500°C a slight grain growth was observed. In the case of initially hot-rolled steel the grain size after deformation was larger than 100 nm.

Thus, the non-equilibrium oversaturated solid solution in 10Mn2VTi steel facilitates additional refinement of microstructure down to nanoscale size during severe plastic deformation.

Stainless steels

Ferritic steel 08Cr18Ti has relatively the same chemical composition as austenitic steel, a higher stacking fault energy and doesn't undergo phase transformations during cold deformation. After severe cold plastic deformation in this steel the submicrocrystalline structure with the grain size of 150–200 nm is formed [10].The least grain size ~ 50 nm is revealed in both austenitic steels having nearly the same hardening H_μ = 7 GPa [10].

By X-ray diffraction analysis, martensitic $\gamma \rightarrow \alpha$ and $\gamma \rightarrow \varepsilon \rightarrow \alpha$ transformations in austenitic steels were observed during cold deformation (Fig. 7) [10].

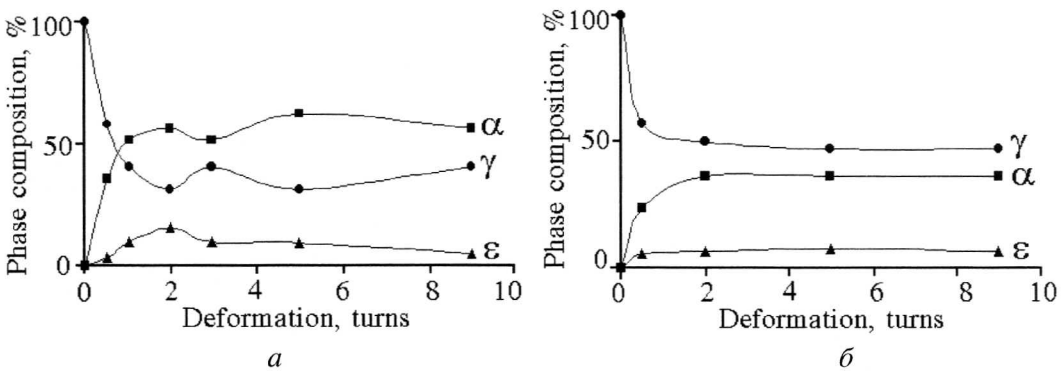

Fig. 7. Martensitic transformations of austenitic steels during SPD by torsion under 6 GPa pressure at 20°C: *a* – 08Cr18Ni10Ti steel; *b* – 05Cr15Ni9Cu2TiNMoV steel

There was ~ 25% of α-martensite and ~ 10% of ε-martensite after preliminary compression of 08Cr18Ni10Ti austenitic steel having in an initial state ~ 10% of δ-ferrite (in Fig. 7,*a* the curve of austenitic fraction includes ~ 10% of δ-ferrite). The following torsion up to $e = 4.9$ (2 revolutions) increases a fraction of the martensite: α-phase – up to ~ 45% and ε-phase – up to ~ 15%. Further, a quantity of ε-martensite decreases a little because of $\varepsilon \rightarrow \alpha$ transformation. There were ~ 50% of α-martensite, ~ 35% of austenite, ~ 10% of δ-ferrite and ~ 5% of ε-martensite in final structure of 08Cr18Ni10Ti steel after $e = 6.4$ (9 revolutions). This state could be considered as two-phase austenitic-martensitic. The transformations don't go up to the end. The intensity of transformations decreases with the increase of strain degree (Fig. 7).

In nitrogen-containing 05Cr15Ni9Cu2TiNMoV steel ~ 35% of α-martensite and ~ 10% of ε-martensite was revealed after torsion with $e = 6.4$ (Fig. 7,*b*).

Thus, it is possible to speak already about two-phase austenitic-martensitic steels.

The most thermostable steel is the austenitic steel with nitrogen. Even at 500°C the grain size in this steel doesn't change and remains less than 100 nm.

Thus, the martensitic transformations in austenitic steels during severe cold deformation by torsion under high pressure promote the additional refinement of structure.

5. Conclusion

The present work shows the possibility of additional refinement of structure up to nanocrystalline state in Al- and Fe-based alloys during SPD by torsion under high pressure due to phase transformations:

– strain aging, with precipitation of θ′- and S′-particles during deformation of Al–Cu–Mg-alloy;

– precipitation of dispersed particles Al_3Sc during deformation of Al–Mg–Sc-alloy;

– carbide transformations during deformation of low-carbon steels;

– martensitic transformations during SPD of austenitic high-alloy steels.

1. *V.M. Segal, V.I. Reznikov, A.E. Drobyshevskiy et al.*, Izv. AN SSSR. Metally № 1, 115 (1981) (in Russian).
2. *N.A. Smirnova, V.I. Levit, V.P. Pilyugin, R.I. Kuznetsov, M.V. Degtyarev*, Fiz. Metal. Metalloved. **62**, 566 (1986) (in Russian).
3. *R.Z. Valiev, A.V. Korznikov, R.R. Mulyukov*, Mater. Sci. Eng. **168**, 141 (1993).
4. *R.Z. Valiev, O.A. Kaibyshev, R.I. Kuznetsov et al.*, DAN SSSR **301**, 864 (1988) (in Russian).
5. *R.Z. Valiev, R.R. Mulyukov, H.Ya. Mulyuko, et al.*, Pis'ma v GTF **15**, vyp. 1, 78 (1989) (in Russian).
6. *V.N. Gridnev, V.G. Gavrilyuk*, Metallofizika **4**, № 3, 74 (1982) (in Russian).
7. *V.V. Sagaradze, S.V. Morozov, V.A. Shabashov et al.*, FMM **66**, Vyp. 2, 328 (1988) (in Russian).
8. *S.V. Dobatkin, V.V. Zakharov, R.Z. Valiev et al.*, Abstracts of NATO ARW "Investigations and Applications of Severe Plastic Deformation", Moscow, August 2–6, 1999, p. 111.
9. *S.V. Dobatkin, V.V. Zakharov, A.Yu. Vinogradov et al.*, Abstracts of the 5-th International Conference on Nanostructured Materials (NANO'2000), Sendai, Japan, August 25–29, 2000, p. 87.
10. *S.V. Dobatkin, R.Z. Valiev, L.M. Kaputkina et al.*, in: Proc. of the Forth Inter. Conf. on Recrystallization and Related Phenomena (REX'99), Tsukuba City, Japan (1999), p. 907–912.
11. *R.I. Kuznetsov, V.I. Bykov, V.P. Chernyshov et al.*, Preprint 4/85, IFM UNS AN SSSR, Sverdlovsk (1985) (in Russian).
12. *T.D. Rostova, V.G. Davydov, V.I. Yelagin, V.V. Zakharov*, Materials Science Forum **331–337**, Part 2, 793 (2000).